



Synthesis and non-parametric evaluation studies on high performance of catalytic oxidation-extraction desulfurization of gasoline using the novel TBAPW₁₁Zn@TiO₂@PAni nanocomposite

Mohammad Reza Khanmohammadi Khorrami | Zahra Shokri Aghbolagh

Department of Chemistry, Faculty of Science, Imam Khomeini International University, Qazvin, Iran

Correspondence

Mohammad Reza Khanmohammadi Khorrami, Department of Chemistry, Faculty of Science, Imam Khomeini International University, Qazvin, Iran. Email: m.khanmohammadi@sci.ikiu.ac.ir

In this work, the new catalyst (assigned as TBAPW₁₁Zn@TiO₂@PAni) was successfully designed and synthesized on the basis of quaternary ammonium salt of zinc monosubstituted phosphotungstate [(n-C₄H₉)₄N][PW₁₁ZnO₃₉] (TBAPW₁₁Zn), titanium dioxide (TiO₂), and polyaniline (PAni). This study reports the catalytic oxidation-extraction desulfurization (ECODS) of sulfur-containing molecules from real and the simulated (Th, BT, and DBT) gasoline using new organic-inorganic hybrid catalyst (TBAPW₁₁Zn@TiO₂@PAni). The ECODS results were shown that the concentration of sulfur compounds (SCs) of real gasoline was lowered from 0.4992 to 0.0122 wt.% with 97% efficiency at 35 °C after 1 h. Furthermore, the synthesized heterogeneous nanocatalyst showed high stability and reusability after five times without significant loss of activity. The high performance of TBAPW₁₁Zn@TiO₂@PAni/H₂O₂/CH₃CO₂H system can be a promising route with a superb potential in the generation of ultra-low-sulfur gasoline. Also the Mann-Whitney U-test results show that there is not a significant difference between the mean of sulfur percentage for DBT & BT, BT & Th and DBT & Th in the presence of the catalyst. Based on the Kruskal-Wallis test results, we can conclude that the temperature, time and amount of catalyst have a significant effect on ECODS efficiency of TBAPW₁₁Zn@TiO₂@PAni nanocomposite.

KEYWORDS

catalytic oxidation-extraction desulfurization, heterogenous catalyst, Polyaniline, Polyoxometalates, titanium dioxide

1 | INTRODUCTION

Presence of high levels of SCs in transportation fuels are an important source causing temperature inversion, global climate changes and acid rain. It is necessary to remove SCs from fuels to avoid SO_x emissions during the burning of petroleum fractions.^[1] In order to fulfill the goal of reducing the air pollution, increasingly

stringent regulations have been imposed to limit the SCs of liquid fuels to a very low level.^[2] In the EU, actually the SCs of gasoline is approximately below 10 ppm.^[3] Hydro desulfurization procedure works at severe operating conditions (at 320–380 °C, 30–70 atm of hydrogen pressure and large reactor volume), and has not ideal performance in removing refractory SCs such as dibenzothiophene (DBT) and their sterically hindered

derivatives.^[4] Oxidative desulfurization has drawn extensive attention as one of the most cost-effective system for elimination of aromatic sulfur-containing compounds under mild operating conditions and it does not require expensive hydrogen.^[5]

The literature related to the selective oxidation of organic sulfur-containing molecules to their corresponding sulfoxides/sulfones through the reaction of hydrogen peroxide and short-chain carboxylic acids introduced it as an effective oxidizing system.^[6,7] Heteropoly Acids (HPAs) as a unique class of anionic metal-oxo clusters has received a lot of attention for catalysis of the ODS process over the past decade.^[8,9] More recently, combined oxidation-extraction desulfurization process (ECODS) is regarded as one of the most appropriate and effective methods due to its unique sulfur removal efficiency.^[10] Among the different varieties of their structures, Keggin HPAs have shown excellent catalytic activity in oxidative desulfurization reactions due to the numerous terminal oxygen atoms.^[11,12] The application and effective separation and reusability of the HPAs-based heterogeneous catalysts are limited because of their high solubility in the polar medium and low specific surface areas.^[13] In order to overcome these drawbacks, the synthesis of HPAs-supported catalysts or complexation with an organic or inorganic cation has been explored in recent years.^[14] Recently, the incorporation of HPAs and TiO₂ has been considered as a promising strategy to enhance the catalytic activity of the metal-oxygen clusters because of its poorly soluble, and low toxicity particles.^[15,16] Furthermore, there has been growing interest in using PANi as a various carrier material for improving the catalytic efficiency of catalysts in heterogeneous system due to its interesting redox properties, easy synthesis route, chemical stability, and low cost.^[17–20] Besides, the incorporation of PANi and inorganic metal oxides have been shown to be a very efficient method to increase the catalytic performance and to improve physical, mechanical, and electrical properties.^[21] All of the above mentioned reasons make the organic PANi polymer and inorganic TiO₂ particles as a promising organic-inorganic hybrid substrate for immobilization of HPAs. Hydrogen peroxide (H₂O₂) is mostly chosen as an environmentally benign oxidant for oxidation of organic compounds due to the only by-product is water.^[22] Aqueous H₂O₂ is not soluble in the oil phase that including SCs. Therefore we carried out the ECODS reaction using phase transfer catalysts to provide a green and effective oxidation process of fuel oil. In other words, in order to facilitate the transition of the HPAs into organic phase, counteraction with quaternary ammonium salt with lipophilic cation was used as a phase transfer agent.

As a part of our continued efforts to improve the HPAs preparation and application,^[23–25] herein we report the synthesis a new type of phase transfer catalyst TBAPW₁₁Zn@TiO₂@PANi as an effective hybrid catalyst for ECODS of real and simulated gasoline. The catalyst was synthesized at ambient temperature and was characterized by elemental analysis, FT-IR, SEM, XRD, UV-Vis, and EDX methods. The mixture of H₂O₂/CH₃CO₂H (in v/v ratio of 2:1) was used as an oxidant and polar acetonitrile utilized as an extraction solvent. Very interestingly, we found that TBAPW₁₁Zn@TiO₂@PANi nanocomposite could oxidize sulfur to sulfoxide and sulfone^[10] under mild conditions. Also, the effect of different factors on the ECODS efficiency, probable oxidation reaction mechanism, the Mann-Whitney U-test and the kinetic of the ECODS process is studied in detail. The TBAPW₁₁Zn@TiO₂@PANi nanocatalyst showed a significant improved catalytic performance in ECODS of gasoline and simulated fuel.

2 | EXPERIMENTAL

2.1 | Materials and analytical characterization

Sodium tungstate dihydrate (Na₂WO₄·2H₂O), disodium phosphate (Na₂HPO₄), zinc nitrate (Zn(NO₃)₂), aniline, ammonium peroxydisulfate ((NH₄)₂S₂O₈), hydrogen peroxide (H₂O₂, 30 vol%), ethanoic acid (CH₃CO₂H), acetonitrile (MeCN) and tetrabutylammonium bromide (TBAB), thiophene (Th), benzothiophene (BT), dibenzothiophene (DBT), and solvent (n-heptane) were obtained Sigma-Aldrich. All aqueous solutions were prepared using double distilled water (DDW). Typical real gasoline (0.7979 g.ml⁻¹ of density at 15 °C, total sulfur content of 0.4992 wt.%) was used. The Fourier transform infrared (FT-IR) spectra were taken with a Thermo-Nicolet-iS10 spectrometer in the range of 400–4000 cm⁻¹ with KBr disks. Ultraviolet visible (UV-vis) spectra were measured with a double beam Thermo-Heylos spectrometer. The surface morphology was analyzed using scanning electron microscope (SEM; LEO 1455 VP). The composition of TBAPW₁₁Zn@TiO₂@PANi composite was also assessed by energy dispersive X-ray analysis measurements (EDX). The X-Ray powder Diffraction (XRD) was performed by D8 Bruker Advanced, X-ray diffractometer using Cu K Alpha radiation ($\alpha = 1.54 \text{ \AA}$) and the data were collected between $2\theta = 5\text{--}80^\circ$. The total sulfur and mercaptan contents in gasoline before and after ECODS reaction were obtained using X-ray fluorescence with a

TANAKA RX-360 SH X-ray fluorescence spectrometer (ASTM D-4294 and D-3227, respectively).

2.2 | Catalytic tests

2.2.1 | Desulfurization of simulated fuel by TBAPW₁₁Zn@TiO₂@PAni catalysts

In order to evaluate the catalytic activity of the synthesized catalyst, simulated fuel was generated through simple mixing of DBT, BT, Th and n-heptane, separately, with the initial SCs of 500 ppm by weight recorded for all of them. The TBAPW₁₁Zn@TiO₂@PAni nanocomposite, H₂O₂/CH₃CO₂H (3 ml) in ratio of 2:1, and simulated fuel was added in a 250-ml round-bottom flask in experimental proportion, which was placed in a thermostatic water bath at particular temperature (25–40 °C) and was stirred vigorously by stirring hot plates. The oxidized SCs were extracted using MeCN in the volume ratio of 1:5 (MeCN/SCs) by a separating funnel. After the ECODS, the upper clear phase (simulated fuel) was analyzed for total sulfur and mercaptan using a TANAKA SIENTIFIC RX-360 SH X-ray fluorescence spectrometer (ASTM D-4294 and D-3227, respectively). The ECODS efficiency of simulated gasoline is calculated simply by the following equation Equation (1), where CS_i and CS_f are initial and final concentration of simulated gasoline after time t, respectively.

$$ECODS \text{ efficiency}\% = \frac{CS_i - CS_f}{CS_i} \times 100 \quad (1)$$

2.2.2 | Desulfurization of real gasoline by TBAPW₁₁Zn@TiO₂@PAni catalysts

In order to verify the ECODS efficiency, similar to the experimental procedure done for the desulfurization

of simulated gasoline, 50 ml of gasoline, 0.1 g of TBAPW₁₁Zn@TiO₂@PAni, 10 ml of MeCN as an extractant and H₂O₂/CH₃CO₂H as an oxidant and in the volume ratio of 2:1 (3 ml) were stirred regularly for 1 hr at 35 °C and were added to round-bottomed flask equipped with stirring hot plates. Consequently, the gasoline was extracted to calculate recovery percentage (for two times reaction: 95 and 94%). The amount of total sulfur and mercaptan content in an oil phase before and after ECODS were determined by a TANAKA SIENTIFIC RX-360 SH X-ray fluorescence spectrometer (ASTM D-4294 and D-3227, respectively). Results for the desulfurization are listed in Table 1.

2.3 | Preparation of catalyst

2.3.1 | Preparation of [(n-C₄H₉)₄N][PW₁₁ZnO₃₉]

[PW₁₁ZnO₃₉]⁹⁻ was synthesized according to the reported methods.^[25–27] Briefly, Na₂WO₄·2H₂O (6 gr), Na₂HPO₄ (6 gr) and Zn (NO₃)₂ (1 gr) were added to 50 ml of DDW, and pH of the mixture was adjusted to 4.7. Based on the literature,^[28] an aqueous solution of TBAB (5 gr in 20 ml) was added drop wise under stirring, and then was heated to 80 °C. Ultimately, the obtained solid was filtered and dried (assigned as TBAPW₁₁Zn).

2.3.2 | Preparation of TBAPW₁₁Zn@TiO₂

In a typical procedure, 0.05 g of TiO₂ was dispersed in 25 ml of acetic acid (2%) then 0.05 g of synthesized TBAPW₁₁Zn was dissolved in 5 ml boiling DDW and added into the reaction vessel slowly. The mixed solution was heated to 60 °C with stirring for 1 hr. After the removal of water through evaporation, a white gel was formed. Then it was aged at 90 °C for 2 hr to obtain a powder form of TBAPW₁₁Zn@TiO₂.

TABLE 1 Catalytic oxidation-extraction desulfurization of gasoline by TBAPW₁₁Zn@TiO₂@PAni

Entry	Properties of gasoline	Unit	Analysis Test Method	Before ECODS	After ECODS ^a
1	Mercaptans	ppm	ASTM D 3227	95	3
2	Total Sulphur Contents	Wt. %	ASTM D 4294	0.4992	0.0122
3	Dynamic Viscosity	@15°C cP	ASTM D 7042	0.79 0.68	0.77 0.66
4	Density by hydrometer	@15°C @20°C g/ml	ASTM D 1298	0.7987	0.7985
5	Surface Tension	@15°C mN/m	ASTM D 1331	20.4	20.3
6	Interfacial Tension	@15°C mN/m	ASTM D 971	18.0	17.8

^aCondition of ODS process: 50 ml of gasoline, 0.10 g of catalyst, 3 ml of oxidant, 10 ml of acetonitrile, reaction temperature = 35 °C, and reaction time = 1 hr.

2.3.3 | Preparation of TBAPW₁₁Zn@TiO₂@PAni catalyst

The TBAPW₁₁Zn@TiO₂@PAni was synthesized by *in situ* chemical oxidation polymerization of aniline monomer in the presence of TBAPW₁₁Zn@TiO₂ solution. In a typical synthesis, 1 ml of aniline and 1 gr of TBAPW₁₁Zn@TiO₂ were added to 60 ml DDW under ultrasonic conditions using an ultrasonic water bath (frequency 35 kHz mains connection 230 V) for 30 min. The polymerization reaction was initiated immediately after the addition of (NH₄)₂S₂O₈ (2.20 g) to the above solution. The mixture was allowed to react for 10 hr under constant stirring. The obtained dark gray solid (TBAPW₁₁Zn@TiO₂) was rinsed thoroughly (3 times) with DDW and finally dried at 70 °C for 4 hr.

2.4 | Computational section

The assumption for the normal distribution is that the mean and the standard deviation reflect the measures related to the central tendency and the dispersion of the studied data, respectively. In distribution-free methods (non-parametric) that are introduced in this study, there are no assumptions about the distribution of the population. Moreover, the non-parametric tests are considered to be the robust methods due to their resistance to outlying observations, which greatly influence on the mean and the standard deviation. In this study, a suitable non-parametric test was selected.

2.4.1 | The Mann–Whitney U-test

The Mann–Whitney U-test is one of the most powerful nonparametric tests used for recognizing two distribution functions. The Mann–Whitney U-test is a strong alternative to the parametric independent-samples t-test. The hypothesis tested by the Mann–Whitney analysis is that the medians of the two groups are equal and no true difference between both samples. In this situation, the ranks for two groups should appear at random. Otherwise, there is a significant difference between the median of two groups. According to this test, first, all the existing data are taken together considered and are ranked. The test allows comparison of the calculated smaller u Equation (2) and (3) with the critical value for U.

$$U_1 = n_1 n_2 + \frac{n_1 (n_1 + 1)}{2} - R_1 \quad (2)$$

$$U_2 = n_1 n_2 + \frac{n_2 (n_2 + 1)}{2} - R_2 \quad (3)$$

3 | RESULTS AND DISCUSSION

3.1 | Characterization studies

Infrared spectroscopy of TBAPW₁₁Zn, TiO₂, PAni and TBAPW₁₁Zn@TiO₂@PAni, are shown in Figures 1, 2 and Table 2. The origins of the vibration peaks are as follows: The characteristic bands of Keggin-type polyoxoanion [TBAPW₁₁Zn] is confirmed by characteristic absorption bands of Zn–O, W–O terminal (W = O_t) and W–O bridging groups (W–O_b–W, W–O_c–W) at 1049, 951, 889, and

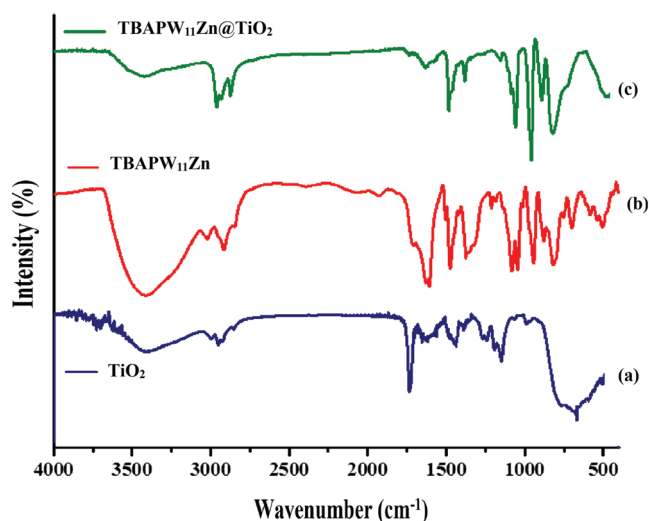


FIGURE 1 FT-IR of a) TiO₂, b) TBAPW₁₁Zn and c) TBAPW₁₁Zn@TiO₂

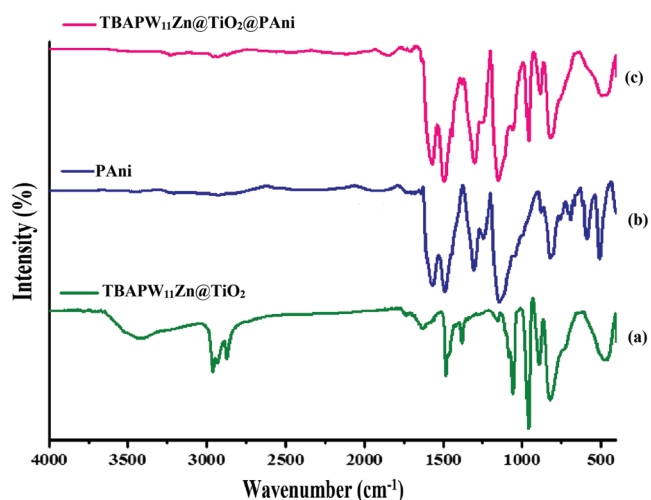


FIGURE 2 FT-IR of a) TBAPW₁₁Zn@TiO₂, b) PAni and c) TBAPW₁₁Zn@TiO₂@PAni

807 cm^{-1} , respectively.^[29] The sharp signal at 1084 cm^{-1} is related to the P–O stretching bonds of the PO_4 tetrahedra (Figure 1b).^[30] As shown in Figure 2(b), pure PANi (emeraldine) salt showed the vibrational frequency at 1522 and 1648 cm^{-1} , which is attributed to the C–C vibration of benzenoid and quinonoid ring, respectively.^[31] The characteristic Keggin-structured bonds were also located distinctively for $\text{TBAPW}_{11}\text{Zn@TiO}_2$ (Figure 1c) and $\text{TBAPW}_{11}\text{Zn@TiO}_2\text{@PAni}$ (Figure 2c). For $\text{TBAPW}_{11}\text{Zn@TiO}_2\text{@PAni}$, four HPAs characteristic peaks appear with only slight shifts compared to the pure $\text{TBAPW}_{11}\text{Zn}$, and the peaks which are observed in the range of 468–702 cm^{-1} and around 1464 cm^{-1} are attributed to the Ti–O bond of TiO_2 indicating the formation of the $\text{TBAPW}_{11}\text{Zn@TiO}_2\text{@PAni}$ hybrid through strong electrostatic interaction.^[15]

The spectrum of $\text{TBAPW}_{11}\text{Zn}$ indicated an intense absorption peak at 255 nm. As shown in PANi spectrum (Figure 3b), the characteristic absorption bands at 242 nm is assigned to the $\pi \rightarrow \pi^*$ transition of the benzenoid ring and the second one in 321 nm is attributed to $n \rightarrow \pi^*$ excitation transition of the quinonoid ring.^[21] The characteristic peak was indicated at 255 nm assigned to $\text{O}^{2-} \rightarrow \text{W}^{6+}$ charge transfer (LMCT) of $\text{TBAPW}_{11}\text{Zn}$ (Figure 3a), 260 nm for $\text{TBAPW}_{11}\text{Zn@TiO}_2\text{@PAni}$ (Figure 3c) which showed slight shifts in the modified synthesized hybrid nanocatalyst. This shifts proved the intermolecular electronic interactions between $\text{TBAPW}_{11}\text{Zn}$, TiO_2 , and PANi. Investigation of the UV–vis spectrum is in good agreement with the results of FT-IR.

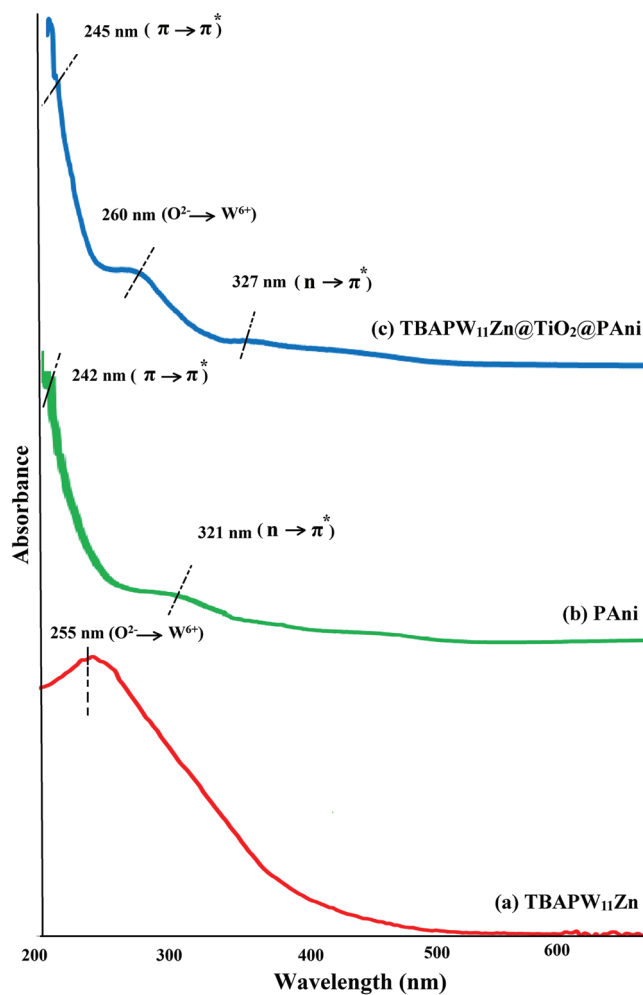


FIGURE 3 The UV–Vis spectra of a) $\text{TBAPW}_{11}\text{Zn}$, b) PANi and c) $\text{TBAPW}_{11}\text{Zn@TiO}_2\text{@PAni}$

TABLE 2 FT-IR peaks of $\text{TBAPW}_{11}\text{Zn@TiO}_2\text{@PAni}$, $\text{TBAPW}_{11}\text{Zn@TiO}_2$ and $\text{TBAPW}_{11}\text{Zn}$

Wavenumber (cm^{-1})			
Compounds			
$\text{TBAPW}_{11}\text{Zn@TiO}_2\text{@PAni}$	$\text{TBAPW}_{11}\text{Zn@TiO}_2$	$\text{TBAPW}_{11}\text{Zn}$	Vibration mode
1031	1038	1049	Stretching of Zn–O
3431–3456	-	-	Stretching of N–H
952	1006	1084	ν (P–O _a)
881	887	889	ν (W = O _i)
830	-	807	ν (W–O _b –W) & ν (W–O _c –W)
1464	1402	-	Anti-symmetric Ti–O–Ti
2852 to 2923	510	-	C–H stretching
505	-	-	C–H out-of-plane bending vibration
1558, 1577–1581, 1481–1485	-	-	Stretching of C=N & C=C
1298–1301, 1242–1245	-	-	Stretching of C–N benzenoid ring
1114–1126	-	-	In-plane bending vibrations of C–H mode of quinonoid (N = Q = N) & benzenoid ring

The X-ray diffraction pattern of TBAPW₁₁Zn, TBAPW₁₁Zn@TiO₂ and TBAPW₁₁Zn@TiO₂@PAni were collected and presented in Figures 4 and 5. The peaks for bulk TBAPW₁₁Zn at 7–10°, and 16–42° showed Keggin-type of HPAs.^[29] The XRD patterns of the PAni showed two broad peaks at 20.2° and 25.4° indicating

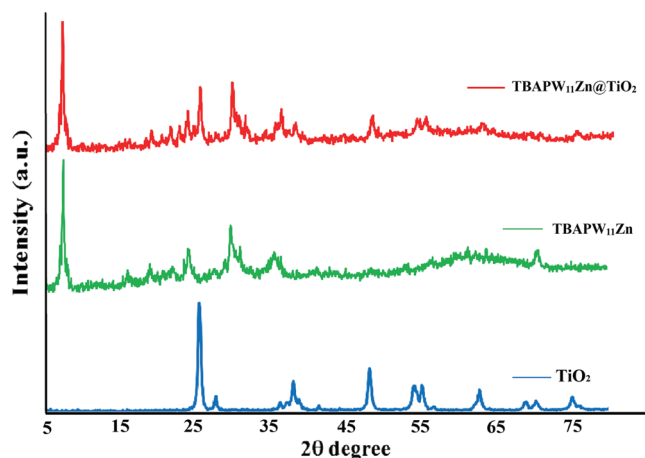


FIGURE 4 XRD pattern of a) TiO₂, b) TBAPW₁₁Zn and c) TBAPW₁₁Zn@TiO₂

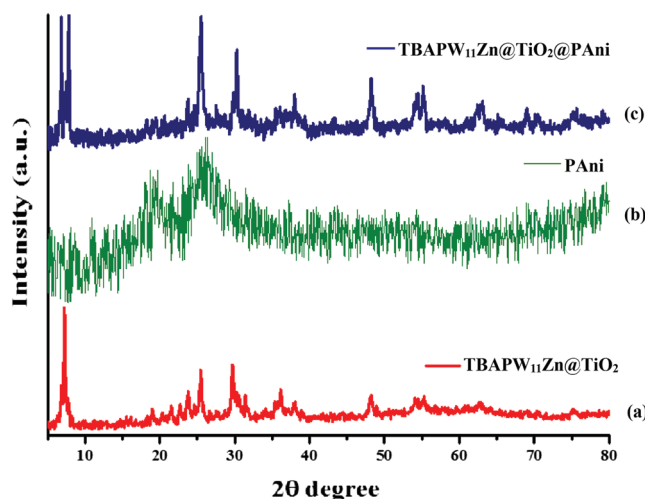


FIGURE 5 XRD pattern of a) TBAPW₁₁Zn@TiO₂, b) PAni and c) TBAPW₁₁Zn@TiO₂@PAni

low degree of crystallinity.^[32] Amorphous nature of PAni is due to the scattering from the PAni chains at interplanar spacing.^[33] As shown in Figure 5, diffraction peaks related to PAni are not detected in the TBAPW₁₁Zn@TiO₂@PAni catalyst. This result indicated that the degree of crystallinity of PAni chain has been hampered in TBAPW₁₁Zn@TiO₂@PAni hybrid.^[33,34] When TBAPW₁₁Zn@TiO₂ nanocomposite are added on the surface of titanium dioxide, due to the restrictive effect of TiO₂ nanoparticles the degree of crystallinity of PAni is compromised.^[35] By comparing the X-ray diffraction patterns of TBAPW₁₁Zn@TiO₂@PAni hybrid nanocatalyst with that of pure TBAPW₁₁Zn, TiO₂ and PAni, it could be found that the sharp peaks at 24.70°, 38.22°, 47.60° and 54.11° are due to (110), (101), (111) and (211) crystal planes of anatase titanium dioxide and HPAs revealed at 7–45° showing the presence of TiO₂ and TBAPW₁₁Zn in PAni.^[36] In addition, the XRD patterns of hybrids TBAPW₁₁Zn@TiO₂@PAni are in good agreement with primary TBAPW₁₁Zn, revealing that the Keggin structure of TBAPW₁₁Zn remains intact in the hybrids (Figure 5c). The crystallite size of TBAPW₁₁Zn@TiO₂@PAni was calculated by the Debye-Scherrer equation Equation (4).

$$D = K \lambda / \beta \cos \theta \quad (4)$$

where D is the average crystallite size, K is equal to 0.89, λ is the wavelength of X-ray (1.5406 Å), β is the Full Width at Half Maximum (FWHM) intensity of the peak, and θ is the half of the diffraction angle.^[37] With respect to equation, the average size of the TBAPW₁₁Zn@TiO₂@PAni nanocomposite is estimated to be about 80.9 nm.

The surface morphology of the sample was recorded by SEM. It is interesting to note that, the SEM images (Figure 6) exhibit sphere-like structures with a mean particle size of ~75 nm for TBAPW₁₁Zn@TiO₂@PAni catalyst.

As evidenced clearly from the EDX results, the presence of the Ti, W and Zn elements in the nanocomposite structure proved the successful synthesis of

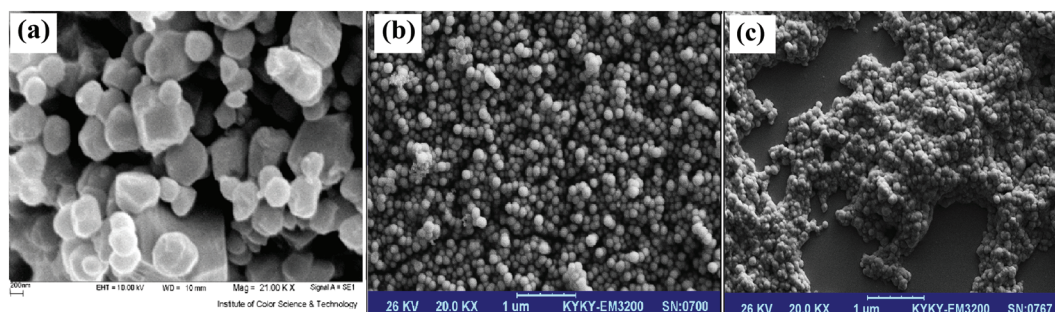


FIGURE 6 SEM images of (a) PAni (b) TiO₂ and (c) TBAPW₁₁Zn@TiO₂@PAni

TBAPW₁₁Zn@TiO₂@PAni (Figure 7). The amounts of Ti, W, Zn, C, N, O and P elements were equal to 30.60, 1.47, 0.07, 19.72, 5.22, 41.86 and 1.07 wt%, respectively. Furthermore, other chemical characterization was recorded by elemental chemical analysis (Table 3).

3.2 | ECODS process results

3.2.1 | Desulfurization of real gasoline

So, in order to prove the superior catalytic activity of TBAPW₁₁Zn@TiO₂@PAni, the exclusion of SCs from real gasoline was performed. It is interesting to note that, the elimination of mercaptan and total sulfur contents from gasoline after desulfurization reaction has a considerable efficiency, while other features of fuel remained unaffected, meaning that the new synthesized composite in this work had superb utilization of CH₃CO₂H/H₂O₂ (see Table 1). X-ray fluorescence spectrometer analysis showed that total SCs (wt %) of gasoline could decrease from 0.4992 wt.% to 0.0122 wt.% and the mercaptans were reached from 95 ppm to 3 ppm. The reason was due to the high performance of TBAPW₁₁Zn@TiO₂@PAni as a catalyst for ECODS system.

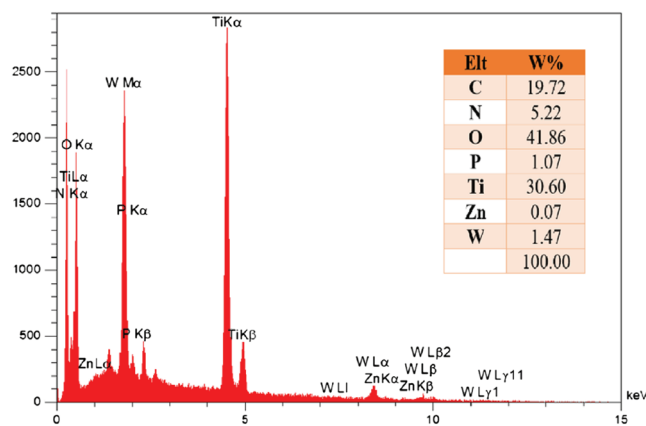


FIGURE 7 EDAX analysis of TBAPW₁₁Zn@TiO₂@PAni

TABLE 3 Elemental analysis of catalysts

Catalyst	Data	K	P	W	Zn	C	N	H
K ₄ [PW ₁₁ ZnO ₃₉]	Calcd (mass%)	5.44	1.08	70.46	2.28	-	-	-
	Exp. (mass%)	5.32	0.98	70.34	2.17	-	-	-
((n-C ₄ H ₉) ₄ N) ₄ [PW ₁₁ ZnO ₃₉]	Calcd (mass%)	-	1.03	67.74	2.19	6.43	0.46	1.21
	Exp. (mass%)	-	0.92	67.63	2.07	6.33	0.35	1.11

3.2.2 | The effect of different sulfur compounds on the ECODS reaction

This study proved the excellent catalytic activity of TBAPW₁₁Zn@TiO₂@PAni in the proprietary elimination of Th, BT, and DBT from n-heptane under the previously mentioned conditions. The oxidation reactivity of the simulated gasoline at the same condition followed the order of DBT > BT > Th, due to the higher electron density of sulfur atom in DBT compared with those in BT and Th. As can be concluded from the literature, the oxidation efficiency of SCs increased with the increase of the electron density of sulfur atom^[20,27]. In the presence of TBAPW₁₁Zn@TiO₂@PAni as catalyst and H₂O₂/CH₃CO₂H as oxidant agent, DBT, BT, and Th are oxidized with 99%, 98%, and 97% efficiencies, respectively.

According to the Figure 8, the presence of H₂O₂/CH₃CO₂H (in v/v ratio of 2:1) as oxidant has a significant effect on the desulfurization efficiency, which is due to the formation of CH₃CO₃H (peroxide acid) as a supplier source of active oxygen.^[37] Also a comparative desulfurization test without CH₃CO₂H (with H₂O₂, 3 ml as oxidant) was shown the negligible conversion of sulfur compounds (see Table 4).

3.2.3 | The effect of the time and temperature on the ECODS reaction

In order to determine the effect of different times and temperatures on the catalytic activity of synthesized catalyst, a series of desulfurization experiments were performed, and the results were presented in Figure 9. Four temperatures were tested (25°, 30°, 35° and 40 °C). It is proved that the activity of present oxidative desulfurization is increased mainly with the increasing temperature. After 1 hr, the desulfurization efficiency from Th, BT and DBT at 35 °C was found to be by 97, 98 and 99% respectively. Based on the results, increasing the process temperature to 40 °C or above did not have a significant effect on the conversion of simulated fuel to their corresponding sulfones. Thus, the temperature of 35 °C was chosen as an optimum temperature in the ECODS system.

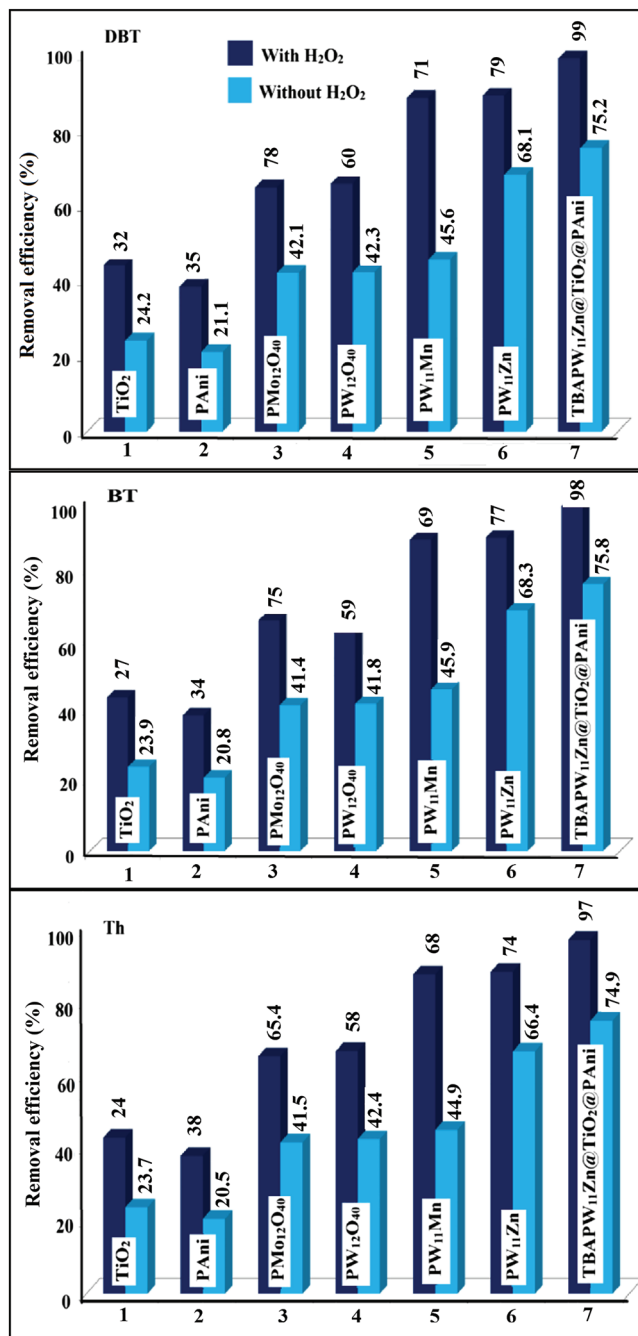


FIGURE 8 The results of ECODS of real gasoline, DBT, BT, and Th with oxidant and without it

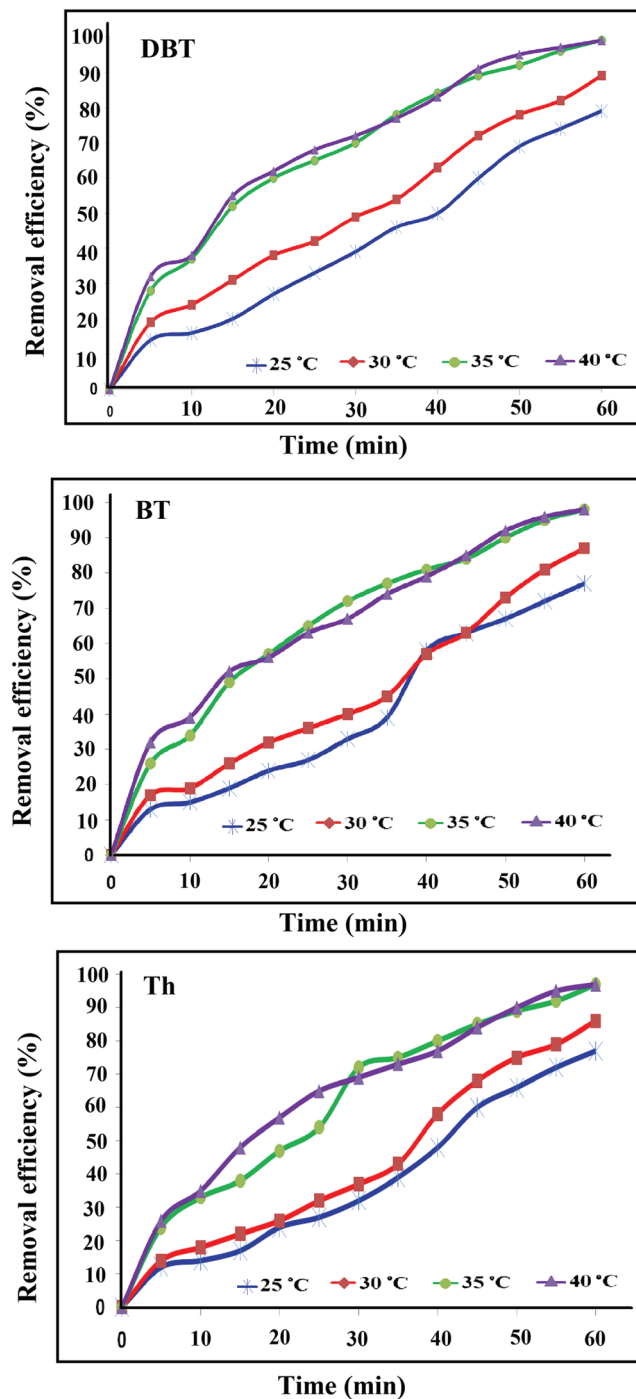


FIGURE 9 Effect of different time and temperature on ECODS of Th, BT and DBT

TABLE 4 Effect of different desulfurization system on sulfur removal from model fuel^a

Entry	Desulfurization system	Sulfur removal%		
		DBT	Th	BT
1	TBAPW ₁₁ Zn@TiO ₂ @P/Ani	75.2	74.9	75.8
2	TBAPW ₁₁ Zn@TiO ₂ @P/Ani/H ₂ O ₂ (3 ml)	93.8	90.8	92.1
3	TBAPW ₁₁ Zn@TiO ₂ @P/Ani/H ₂ O ₂ /CH ₃ CO ₂ H (in v/v ratio of 2:1)	99	97	98

^aCondition of ODS process: 50 ml of model fuel (500 ppmw of Th, BT, and DBT in *n*-heptane), 0.10 g of catalyst, 10 ml of acetonitrile, reaction temperature = 35 °C, and reaction time = 1 hr.

3.2.4 | The effect of the catalyst amounts on the ECODS reaction

As can be seen in Table 5, the amount of catalyst has a significant effect on the sulfur removal efficiency. Furthermore, the conversion of simulated fuel into their corresponding sulfones was enhanced quickly along with the reaction time. Amount of catalyst was optimized by changing it from 0.02 gr to 0.12 gr. When 0.1 gr of TBAPW₁₁Zn@TiO₂@PAni was applied maximal sulfur removal was achieved. In the same manner, 13, 15, 16 and 13% of Th, BT, DBT and gasoline were eliminated in the absence of catalyst as a blank test. When the concentration level of the catalyst was enhanced to 0.12 g, no significant changes were found in desulfurization rate. The reason may be due to the prevention of sulfide adsorption and oxidation onto catalyst due to the accumulation of the metal-oxo and metal-peroxo species. Ultimately, 0.1 gr of catalyst was chosen as a suitable amount in the ECODS reaction system.

3.2.5 | The effect of different catalysts on the ECODS reaction

As a comparison, the effect of various HPAs-based catalysts on the removal of SCs content in the desulfurization reaction was evaluated and the results were listed in Table 6. Blank test was carried out in the absence of TBAPW₁₁Zn@TiO₂@PAni as a catalyst. It was found that in the absence of catalysts % conversion was very low. With respect to the results, TBAPW₁₁Zn is more effective than K₃PW₁₂O₄₀ (Table 6, entry 3) and K₃PMO₁₂O₄₀ (Table 6, entry 2) samples. Also, the ability of pure TiO₂ in removal of total sulfur content was found negligible (Table 6, entry

TABLE 5 Effect of Catalyst dosage on the ECODS of simulated and actual gasoline^a

Entry	Amount of catalyst (gr)	Conversion (%)			
		Actual Gasoline	DBT	BT	Th
1	0 (Blank)	13	16	15	13
2	0.02	27	32	29	27
4	0.04	46	48	47	45
6	0.06	60	71	68	67
8	0.08	89	90	90	88
10	0.1	98	99	98	97
12	0.12	98	90	98	97

^aCondition of ODS process: 50 ml of actual gasoline and simulated gasoline (500 ppmw of Th, BT, and DBT in *n*-heptane), 0.10 g of catalyst, 3 ml of oxidant, 10 ml of acetonitrile, reaction temperature = 35 °C, and reaction time = 1 hr.

TABLE 6 Effect of different catalysts in oxidation desulfurization of different sulfur compounds^a

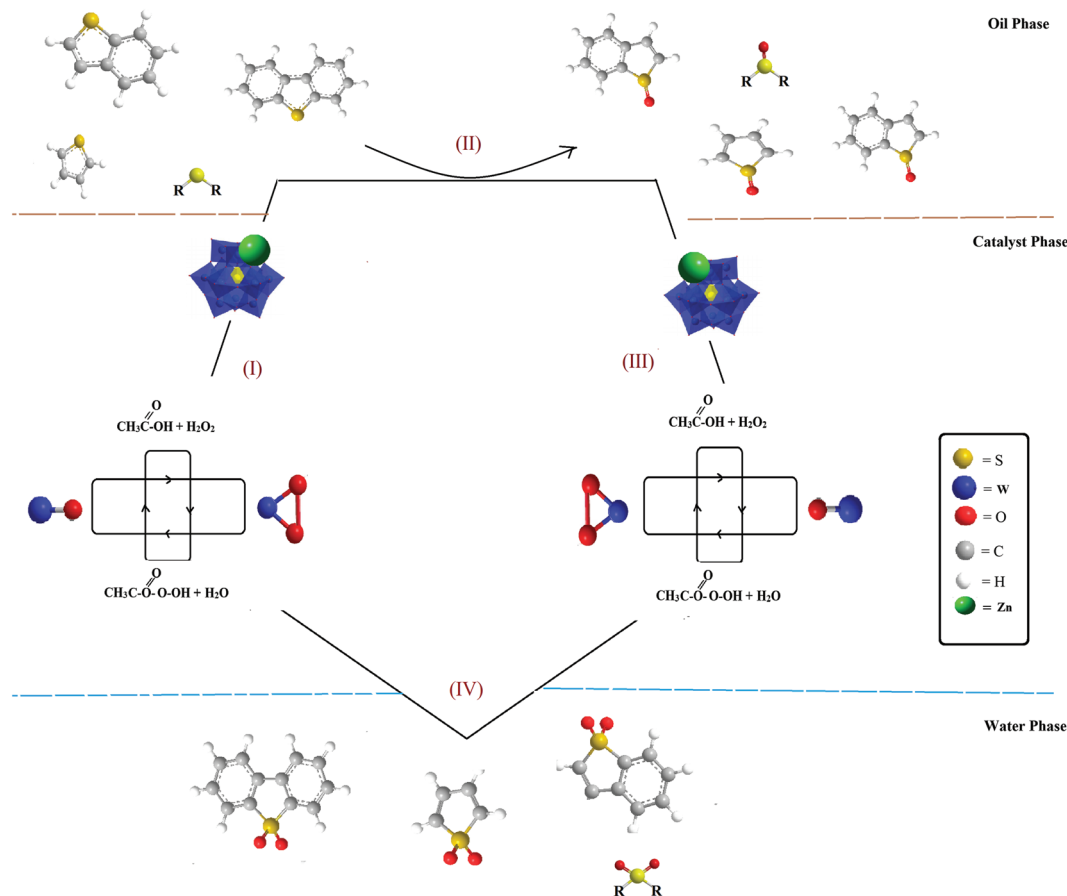
Entry	Catalyst	Conversion %			Ref.
		DBT	Th	BT	
1	H ₇ SiV ₃ W ₉ O ₄₀	92	-	93	[37]
2	H ₃ PMO ₁₂ O ₄₀	78	-	75	[37]
3	K ₃ PW ₁₂ O ₄₀	60	58	59	[38]
4	K ₄ SiW ₁₂ O ₄₀	58	56	56	[38]
5	H ₆ P ₂ W ₁₈ O ₆₂	58	-	52	[37]
6	PMo@HKUST-1	95	90	-	[39]
8	HPMo@SiO ₂	97	-	-	[40]
9	HPW-TiO ₂ -SiO ₂	96	-	-	[19]
10	PAni	35	38	34	[19]
11	PW ₁₁ Mn/NiO/PAN	98	97	98	[19]
12	CTAB-PTA@CS	95	92	93	[21]
13	PW ₁₁ Zn@TiO ₂	94	91	92	This Work
14	TBAPW ₁₁ Zn	79	74	77	This Work
15	TiO ₂	32	24	27	This Work
16	TBAPW ₁₁ Zn@TiO ₂ @PAni	99	97	98	This Work
17	Blank Test	16	13	15	This Work
18	TBA-SiW ₁₂ O ₄₀	61	59	60	[36]
19	TBA-Si ₂ W ₁₈ Mn ₄	69	66	68	[36]
20	PW ₁₁ Mn	71	69	68	[19]

^aCondition of ODS process: 50 ml of gasoline or model fuel (500 ppmw of Th, BT, and DBT in *n*-heptane), 0.10 g of catalyst, 3 ml of oxidant, 10 ml of acetonitrile, reaction temperature = 35 °C, and reaction time = 1 hr.

15), although the synthesized TBAPW₁₁Zn@TiO₂@PAni composite is demonstrated significant performance in ECODS process. Fortunately, among all the catalytic desulfurization experiments, the ECODS reaction with TBAPW₁₁Zn@TiO₂@PAni composite showed the highest catalytic efficiency (Table 6, entry 16).

3.2.6 | The suggested mechanism of the oxidative desulfurization

In order to get an insight into the ECODS reaction, we propose a mechanism for the activation of HPAs-based catalyst which was put forward. As shown in Scheme 1, peracetic acid (CH₃CO₃H) is generated due to reaction of hydrogen peroxide and glacial acetic acid as an active oxygen source. In a second step, W=O of the TBAPW₁₁Zn is turned into the active W-peroxide species (W (O₂)) and along with the reaction the oxygen is donated from CH₃CO₃H. The W (O₂) species oxidize the SCs, faster than the W=O. Then, oxygen donated from W (O₂) is transferred to Th, BT, and DBT and the formation of



SCHEME 1 Suggested mechanism of the oxidative desulfurization by using $\text{CH}_3\text{COOH}/\text{H}_2\text{O}_2$ as oxidant agent.

the transition states are thiophene sulfoxide (ThO), benzothiophene sulfoxide (BTO), and dibenzothiophene sulfoxide (DBTO). Then, W-peroxide is turned to $\text{W}=\text{O}$ and reacts with $\text{CH}_3\text{CO}_3\text{H}$ again for the next step. The ThO, BTO, DBTO are oxidized by W (O_2) and ThO_2 , BTO_2 , DBTO_2 ^[10] are generated and the W-peroxide is regenerated.^[22,38] Therefore, the oxidation mechanism of simulated oil and process of the desulfurization are verified.

3.2.7 | Kinetics of oxidation reaction of DBT, BT and Th

The conversion results for the ECODS process were appeared to obey the first-order kinetic model. The kinetics of oxidation of was investigated under multiple conditions of experimental temperature ranging 25, 30, 35 and 40 °C. It is critical to note that, by increasing experimental temperature from 25 to 35 °C, removal of Th from 73 to 97%, BT from 74 to 97% and for DBT from 75 to 98% in 1 h is increased. The rate constant (k) was estimated as follows Equation (7), on the basis of the first-order kinetics:

$$-\frac{dC}{dt} = kC \quad (6)$$

$$\int_{C_0}^C \frac{dC}{C} = \ln \frac{C}{C_0} = -kt \quad (7)$$

Communication between C and t can be defined by equation (8):

$$C = C_0 e^{-kt} \quad (8)$$

In this equation, C_0 and C_t are the initial concentrations and concentrations at time t , respectively. As shown in Figure 10 and Equation 8, a linear relationship was observed between (C/C_0) and t . The correlation was achieved close to unity (Table 7). The results approved that the oxidation reaction kinetics fitted to the pseudo-first-order model. Moreover, the affiliation of k on the reaction temperature could be expressed by the well-known Arrhenius equation (Equation 9).^[22]

$$k = A e^{(-E_a/RT)} \quad (9)$$

In the above equation, A is the Arrhenius frequency

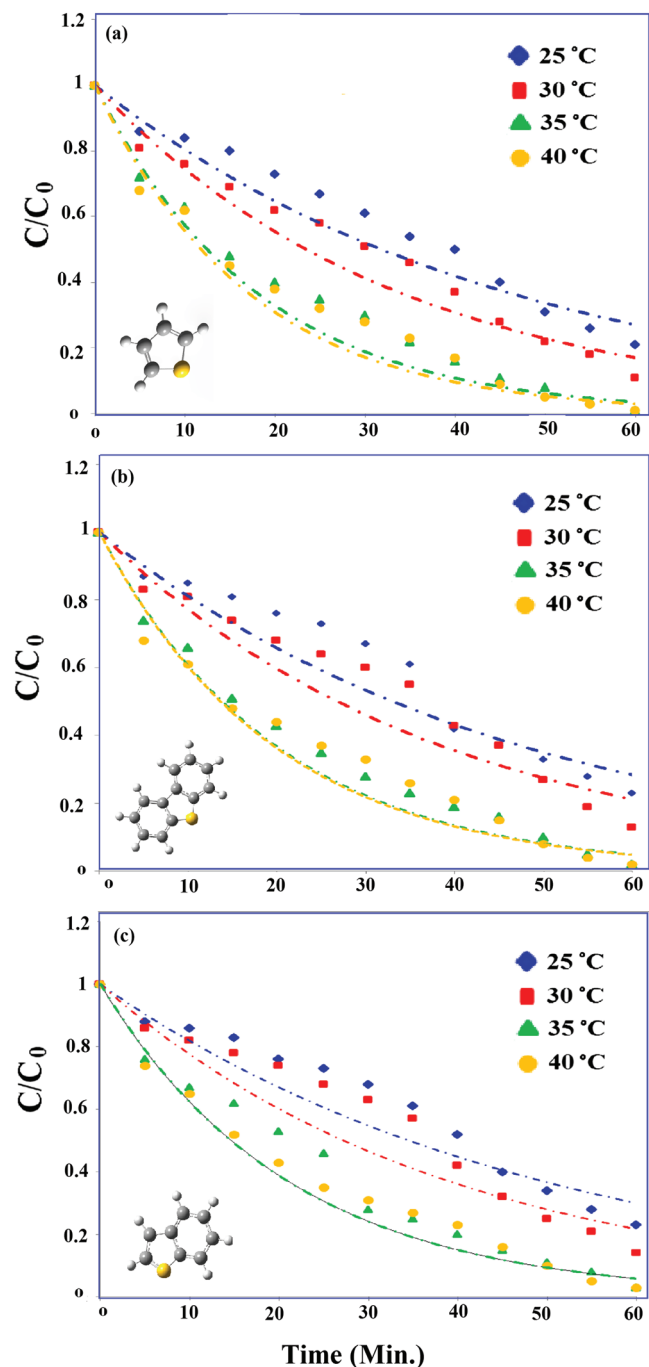


FIGURE 10 Plots of C/C_0 for the oxidation of a) Th, b) DBT and c) BT

factor, E_a is the apparent activation energy, R is the universal gas constant and, T is the reaction temperature (in Kelvin) [38]. It should be noted that, the Arrhenius curves and the apparent activation energy (E_a) for the ECODS of DBT, BT and Th equal to were 49.511, 52.677 and 55.708 $\text{kJ}\cdot\text{mol}^{-1}$, respectively (see Figure 11 and Table 7). The efficiency of the ECODS process for model gasoline was increased in the order of $\text{DBT} > \text{BT} > \text{Th}$. The reason

TABLE 7 Pseudo-first-order rate constants and correlation factors of the S-PAC (Th, BT and DBT)

Temperature (°C)	Rate constant k (min^{-1})			Correlation factor R^2		
	Th	BT	DBT	Th	BT	DBT
25	0.019	0.021	0.022	0.912	0.918	0.923
30	0.024	0.025	0.030	0.877	0.889	0.921
35	0.047	0.045	0.056	0.917	0.917	0.874
40	0.047	0.050	0.059	0.917	0.947	0.890

behind this behavior is due to the lowest aromatic p-electron density on the Th sulfur atom compared to those in DBT and BT.

3.2.8 | Regeneration of catalyst phase

The long-term stability of the $\text{TBAPW}_{11}\text{Zn@TiO}_2\text{@PAni}$ catalyst has remarkable importance for its industrial performance. To obtain further insight into the regeneration of the $\text{TBAPW}_{11}\text{Zn@TiO}_2\text{@PAni}$ composite in the ECODS process of DBT compounds, the following experiments were done. Briefly in a typical reaction, the water catalyst phase was reused in five consecutive experiments by filtration; it was washed and dried at 25 °C. After test, the desulfurization efficiency of the catalyst decreases slightly from 99% in the first cycle to 94% in the fifth cycle (The results are presented in Figure 12). Due to the product accumulation and the decrease in pH value, we observed the slight decrease in ECODS efficiency of the catalyst system. Also, the oxidation product was reextracted by dichloromethane. As Figure 13 the infrared spectroscopy had been proven to be DBT sulfone (DBTO_2).^[39]

3.3 | Computational results and discussion

3.3.1 | The effect of the catalyst amounts on the ECODS reaction

The introduced catalyst in the ECODS process is not influenced by the structure of the sulfur-containing compounds. In other words, the synthesized catalyst ($\text{TBAPW}_{11}\text{Zn@TiO}_2\text{@PAni}$) provides the possibility for performing the ECODS on various sulfur-containing compounds. In order to prove this, the Mann-Whitney U-test were performed in different dosages of catalyst (0, 0.02, 0.04, 0.06, 0.08, 0.1 and 0.12), and the results are as follows:

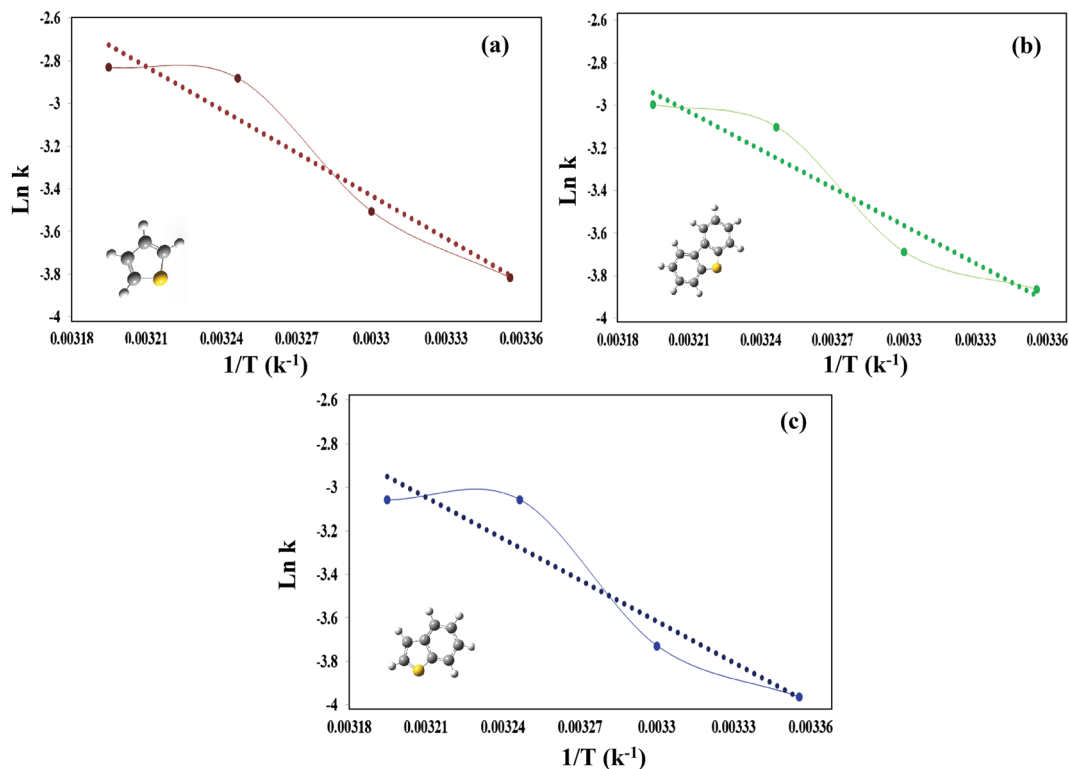


FIGURE 11 Arrhenius plot for the oxidation of a) Th, b) DBT and c) BT

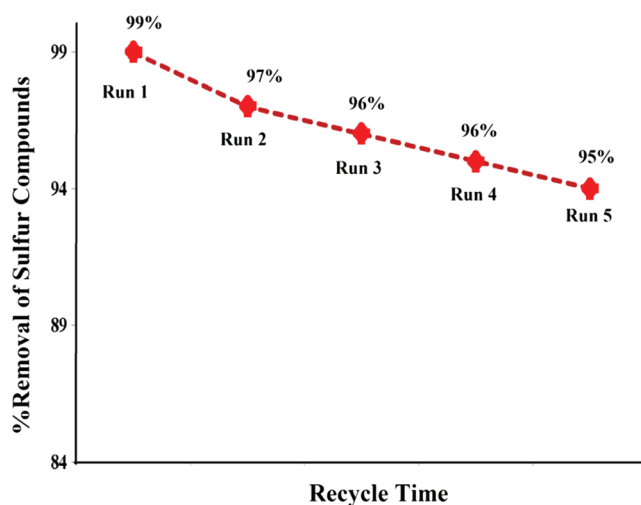


FIGURE 12 Effect of the recycle times on the ECODS efficiency by TBAPW₁₁Zn@TiO₂@PAni

The Mann–Whitney U-test for SCs

Table 8 shows the comparison for the smaller of U test values of the following two test-statistics with the critical value of U. The smaller of U test values for DBT & BT, BT & Th and DBT & Th are equal to 20.5, 20.0 and 20.0, respectively. As shown in Table 8, for a two-sided test with $n_1 = n_2 = 7$, the 5% level of U is equal to 8. Thus, the null hypothesis (symbolized by H_0) is accepted and it can be concluded that, there is no evidence to prove the difference between the two comparison groups.

Additionally, it can be proved that, there is not a significant difference between the mean of sulfur percentage for DBT & BT, BT & Th and DBT & Th in the presence of the catalyst.

3.3.2 | The effect of the time and temperature on the ECODS reaction

The Kruskal–Wallis analysis of SCs

The H_0 was tested by the Kruskal–Wallis test upon which, it is stated that the three instruction methods have the same effect on the number of correct responses achieved.^[41] Thus, the samples are selected randomly from the equal population distribution. The calculated Kruskal–Wallis statistic is explicated as a chi-square value and it is represented to be significant at $p < 0.1$, and for DBT, BT and Th, the value of χ^2 ($df = 2$) is equal to 4.74, 4.76 and 5.00, respectively. According to the number of correct responses calculated, it was found that the three methods are not similarly effective (because as shown in Table 9, the value of 4.61 is less than the values of 4.74, 4.76 and 5.00), therefore, the H_0 is rejected. Thus, it was found that the temperature, time and amount of catalyst have a significant effect on ECODS efficiency of TBAPW₁₁Zn@TiO₂@PAni nanocomposite.

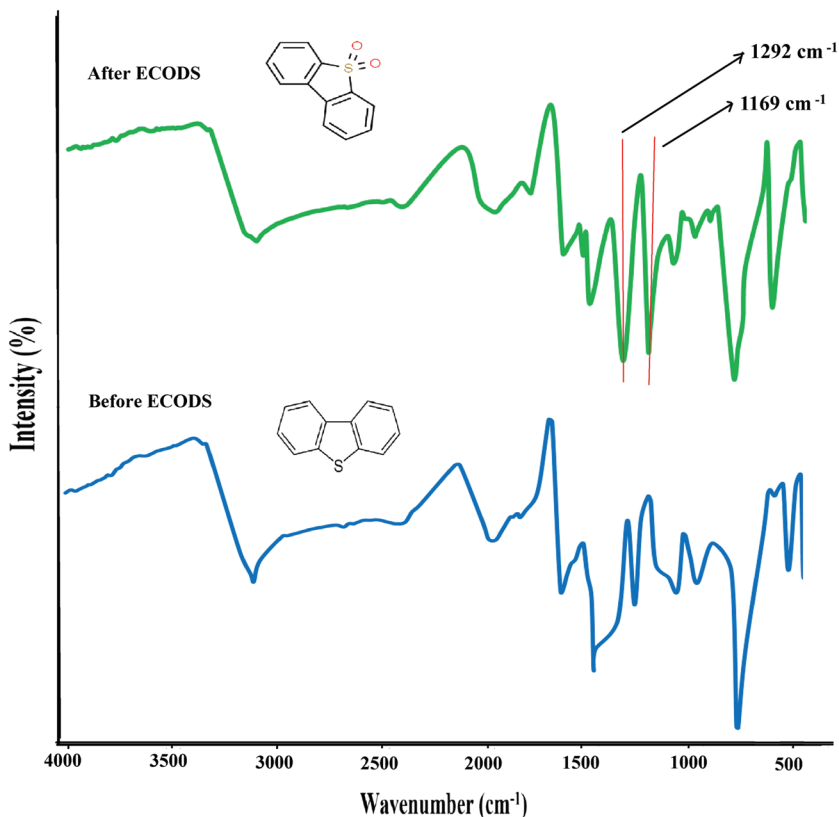


FIGURE 13 FT-IR spectrum for the DBT before and after desulfurization process

TABLE 8 The smaller of U test values for S-PAC

n_2/n_2	Critical values of U	The smaller of U test values		
		DBT & BT	BT & Th	DBT & Th
7*7	8	20.5	20.0	20.0

TABLE 9 The obtained Kruskal-Wallis of S-PAC

df	A	Critical values of Chi-square	Calculated values of Chi-square			p		
			Th	BT	DBT	Th	BT	DBT
2	0.100	4.61	5.00	4.76	4.74	$p < 0.1$	$p < 0.1$	$p < 0.1$

4 | CONCLUSIONS

In this study, we describe the activation behavior of a TBAPW₁₁Zn@TiO₂@PAni nanocomposite for the oxidative desulfurization of SCs from simulated and real gasoline. The SCs is oxidized mainly to water-soluble polar compounds, such as sulfoxide and sulfone, which are in situ extracted into the water catalyst phase. The TBAPW₁₁Zn@TiO₂@PAni hybrid demonstrated excellent catalytic activity and selectivity in the ECODS system. Moreover, we could display that the nanocomposite can

be reused for at least five cycles without a consequential decrease in the catalytic activity in the oxidative desulfurization of SCs.

ACKNOWLEDGMENTS

The authors are grateful for financial supported by the Iran National Science Foundation: INSF 97000426. Also, the First author of this paper gratefully acknowledges the support from department of Food Science and Agricultural Chemistry, Macdonald Campus, McGill University and special thanks Dr. Ashraf Ismail for providing research facilities.

ORCID

Zahra Shokri Aghbolagh  <https://orcid.org/0000-0002-0255-9567>

REFERENCES

- [1] B. Bertleff, J. Claußnitzer, W. Korth, P. Wasserscheid, A. Jess, J. Albert, *ACS Sustainable Chem. Eng.* **2017**, 5, 4110.
- [2] S. Iwao, Y. Baba, *Carbon* **2016**, 98, 115.
- [3] B. Bertleff, R. Goebel, J. Claußnitzer, W. Korth, M. Skiborowski, P. Wasserscheid, A. Jess, J. Albert, *ChemCatChem* **2018**, (20), 4602.
- [4] H. Zhang, J. Gao, H. Meng, C. X. Li, *Ind. Eng. Chem. Res.* **2019**, 19, 6658.

- [5] W. Jiang, L. Dong, H. Li, H. Jia, L. Zhu, W. Zhu, H. Li, *J. Mol. Liq.* **2019**, 274.
- [6] S. Otsuki, T. Nonaka, N. Takashima, W. Qian, A. Ishihara, T. Imai, T. Kabe, *Energy Fuels* **2000**, (6), 1232.
- [7] M. A. Rezvani, Z. Shokri Aghbolagh, H. Hosseini Monfared, S. Khandan, *J. Ind. Eng. Chem.* **2017**, 52, 42.
- [8] J. Tong, W. Wang, L. Su, Q. Li, F. Liu, W. Ma, Z. Lei, L. Bo, *Catal. Sci. Technol.* **2017**, 1, 222.
- [9] J. J. Walsh, A. M. Bond, R. J. Forster, T. E. Keyes, *Coord. Chem. Rev.* **2016**, 306, 217.
- [10] W. Jiang, H. Jia, H. Li, L. Zhu, R. Tao, W. Zhu, H. Li, S. Dai, *Green Chem.* **2019**, 21, 3074.
- [11] G. Wang, D. Wang, X. Xu, L. Liu, F. Yang, *J. Hazard. Mater.* **2012**, 217, 366.
- [12] F. Banisharif, M. R. Dehghani, J. M. Campos-Martin, *Energy Fuels* **2017**, 5, 5419.
- [13] M. Chamack, A. R. Mahjoub, H. Aghayan, *Chem. Eng. J.* **2014**, 255, 686.
- [14] X. Liao, D. Wu, B. Geng, S. Lu, Y. Yao, *RSC Adv.* **2017**, (76), 48454.
- [15] M. A. Rezvani, A. Fallah Shojaie, M. H. Loghmani, *Catal. Commun.* **2012**, 25, 36.
- [16] H. Shi, M. Ruth, C. Vincent a, Z. Jinshun, *Part. Fibre. Toxicol.* **2013**, 10, 15.
- [17] L. Ni, G. Yang, C. Sun, G. Niu, Z. Wu, C. Chen, X. Gong, C. Zhou, G. Zhao, J. Gu, W. Ji, *Mater. Today Energy* **2017**, 6, 53.
- [18] B. K. Kuila, B. Nandan, M. Böhme, A. Janke, M. Stamm, *Chem. Commun.* **2009**, (38), 5749.
- [19] K. Zhang, L. L. Zhang, X. S. Zhao, J. Wu, *Chem. Mater.* **2010**, 4, 1392.
- [20] M. A. Rezvani, M. Shaterian, Z. Shokri Aghbolagh, R. Babaei, *Environ. Prog. Sustainable Energy* **2018**, (6), 1891.
- [21] M. A. Rezvani, O. Feghhe Miri, *Chem. Eng. J.* **2019**, 369, 775.
- [22] J. Zongxuan, L. Hongyinga, Z. Yongna, L. Can, *Chin. J. Catal.* **2011**, 32, 707.
- [23] M. A. Rezvani, M. Alinia Asli, S. Khandan, H. Mousavi, Z. Shokri Aghbolagh, *Chem. Eng. J.* **2017**, 312, 243.
- [24] R. Hajian, F. Jafari, *J. Iran. Chem. Soc.* **2018**, 1, 1.
- [25] D. Julião, A. C. Gomes, M. Pillinger, L. Cunha-Silva, B. de Castro, I. S. Gonçalves, S. S. Balula, *Fuel Process. Technol.* **2015**, 131, 78.
- [26] O. A. Kholdeeva, M. P. Vanina, M. N. Timofeeva, R. I. Maksimovskaya, T. A. Trubitsina, M. S. Melgunov, E. B. Burgina, J. Mrowiec-Bialon, A. B. Jarzebski, C. L. Hill, *J. Catal.* **2004**, 2, 363.
- [27] J. S. Beck, J. C. Vartuli, W. Jelal Roth, M. E. Leonowicz, C. T. Kresge, K. D. Schmitt, C. T. W. Chu, et al., *J. Am. Chem. Soc.* **1992**, (27), 10834.
- [28] J. A. F. Gamelas, A. M. V. Cavaleiro, E. de Matos Gomes, M. Belsley, E. Herdtweck, *Polyhedron* **2002**, (25), 2537.
- [29] Z. Nadealian, V. Mirkhani, B. Yadollahi, M. Moghadam, S. Tangestaninejad, I. Mohammadpoor-Baltork, *J. Coord. Chem.* **2013**, (7), 1264.
- [30] H. Yang, T. Song, L. Liu, A. Devadoss, F. Xia, H. Han, H. Park, W. Sigmund, K. Kwon, U. Paik, *J. Phys. Chem. C* **2013**, (34), 17376.
- [31] S. Wang, Z. Tan, Y. Li, L. Sun, T. Zhang, *Thermochim. Acta* **2006**, 2, 191.
- [32] A. Olad, S. Behboudi, A. Akbar Entezami, *Bull. Mater. Sci.* **2012**, (5), 801.
- [33] C. Lai, H. Z. Zhang, G. R. Li, X. P. Gao, *J. Power Sources* **2011**, 10, 4735.
- [34] H. Xia, Q. Wang, *Chem. Mater.* **2002**, 5, 2158.
- [35] P. Rajakani, C. Vedhi, *Int. J. Ind. Chem.* **2015**, 4, 247.
- [36] A. S. Danial, M. M. Saleh, S. A. Salih, M. I. Awad, *Power Sources* **2015**, 293, 101.
- [37] M. A. Rezvani, Z. Shokri Aghbolagh, H. Hosseini Monfared, *Appl. Organomet. Chem.* **2018**, (12), e4592.
- [38] A. F. Shojaei, M. A. Rezvani, M. H. Loghmani, *Fuel Process. Technol.* **2014**, 118, 1.
- [39] L. Hao, M. Wang, W. Shan, C. Deng, W. Ren, Z. Shi, H. Lü, *J. Hazard. Mater.* **2017**, 339, 216.
- [40] M. A. Rezvani, M. Shaterian, F. Akbarzadeh, S. Khandan, *Chem. Eng. J.* **2018**, 333, 537.
- [41] X. Yan, J. Yan, P. Mei, J. Lei, *J. Wuhan. Univ. Technol. Mat. Sci. Edit.* **2008**, 6, 834.

How to cite this article: Khanmohammadi Khorrami MR, Shokri Aghbolagh Z. Synthesis and non-parametric evaluation studies on high performance of catalytic oxidation-extraction desulfurization of gasoline using the novel TBAPW₁₁Zn@TiO₂@PAni nanocomposite. *Appl Organometal Chem.* 2019;e5299. <https://doi.org/10.1002/aoc.5299>